CONTROL OF AN ARTIFICIAL MOUTH PLAYING A TROMBONE AND ANALYSIS OF SOUND DESCRIPTORS ON EXPERIMENTAL DATA

Nicolas Lopes, Thomas Hélie, René Caussé

CONTROL OF AN ARTIFICIAL MOUTH PLAYING A TROMBONE AND ANALYSIS OF SOUND DESCRIPTORS ON EXPERIMENTAL DATA

Nicolas Lopes
IRCAM-CNRS-UPMC, UMR 9912,
1 place Igor Stravinsky,
75004 Paris, France
nicolas.lopes@ircam.fr

Thomas Hélie
IRCAM-CNRS-UPMC, UMR 9912,
1 place Igor Stravinsky,
75004 Paris, France
thomas.helie@ircam.fr

René Caussé
IRCAM-CNRS-UPMC, UMR 9912,
1 place Igor Stravinsky,
75004 Paris, France
rene.causse@ircam.fr

ABSTRACT

This paper deals with a robotized artificial mouth adapted to brass instruments. A technical description of the robotic platform is drawn, including calibrations, initialization processes, and modes of control. An experimental protocol is proposed and the repeatability is checked. Then, experiments are conducted on a trombone for several types of quasi-static controls. Sound descriptors (fundamental frequency, roughness, energy) of measured acoustic signals are estimated and used to build cartographies indexed by the control inputs. An analysis reveals that several stable notes can easily be reached using a basic mapping with respect to these control inputs. However, a histogram of fundamental frequencies shows that some notes in the high range that can be played by musicians are not reached by the artificial mouth. It also reveals that some notes are difficult to play in the middle range. This exploration suggests some possible improvements of the machine that are finally discussed.

1. INTRODUCTION

Brass wind instruments are self-sustained musical instruments. Their self-oscillations are due to the non-linearity of the aero-elastic valve, namely, the jet coupled to the lips, which is loaded by the acoustic resonator. But, although the musician's control of the valve is crucial, it is very difficult to study this bio-physical system and to make "in vivo" measurements. For this reason, artificial mouths have been developed, see e.g. [1–5].

This paper deals with a robotized version a such systems. This robotization was initiated during the CONSONNES project [6]. It also involved mechatronic projects in an engineering school [7] and several internships [8–11]. Some first results and evolutions of the machine functionalities have been presented in [12–14]. In the last one, it has been showed that sequences of a few trumpet notes could be played with a simple open loop control, using a "hand-tuned" mapping based on a sound descriptor analysis [1] .

[1] A movie can been downloaded on the following website:
http://recherche.ircam.fr/anasyn/helie/Brasstronics/FilmBrasstronics2011.avi

In this paper, a systematic approach is proposed and based on (1) calibrations and initialization processes, (2) an experimental protocol and repeatability tests, and (3) sets of cartographies of sound descriptors (with respect to quasi-static inputs) for several modes of control. It allows characterizing notes that can be easily played, and to exhibit some limitations of the machine as well as some dyssymmetry between the lips.

This paper is organized as follows. Section 2 gives an overview of the robotic platform, its sensors and actuators. Section 3 is devoted to the calibration of some sensors and to the configuration of the machine. This includes initialization processes and feedback-loop controller settings. In section 4, an experimental protocol is proposed and the repeatability is checked. Then, the first experimental results obtained for a single control variable are presented in section 5. They allow the establishment of a partial but robust mapping based on a sound descriptor analysis. Section 6 extends these results to 2D cartographies for various control modes with multiple inputs. In particular, the playing frequencies of the set of all cartographies are examined and compared to the impedance peaks of the trombone. This analysis suggests some possible improvements of the machine that are discussed in section 7 with conclusions and perspectives.

2. TECHNICAL DESCRIPTION

The robotic platform is composed of three principal parts : (1) the air supply, (2) the artificial mouth with two lips and (3) the brass instrument with artificial fingers. It includes a set of height actuators, fourteen sensors, interfaced with a DSP setup and a computer to control the machine.

2.1 Mechanical parts

The mouth (M) is a $\simeq 80cm^3$ chamber, which is fed by a controlled air supply. It is ended by two vertical artificial lips (L_1, L_2). Each lip is a cylindrical latex chamber filled of water. The brass instrument (in this work, a valve trombone) with its mouthpiece (MP) is fixed close to the mouth. The contact of the lips with the mouthpiece is ensured by controlling the position of the (mobile) mouth. Three artificial fingers can be used to push on the trombone valves. These components and their coupling are represented in figure 1.

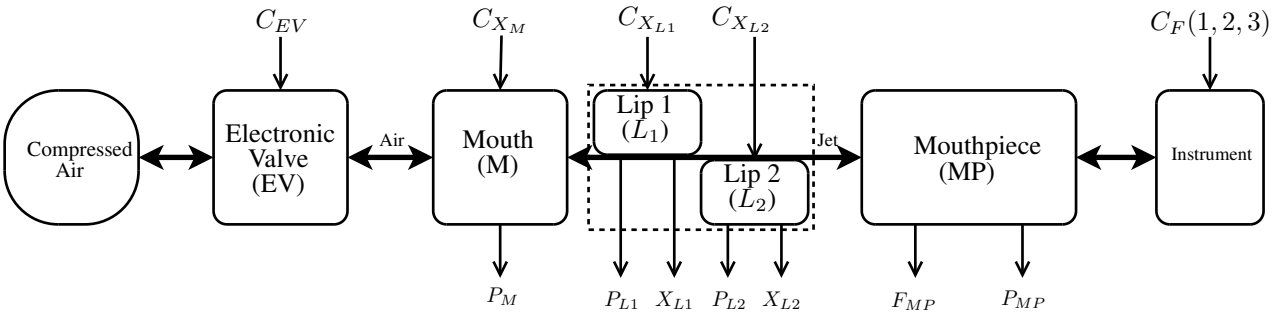

Figure 1. Block diagram of the robotized platform.

2.2 Actuators

The input airflow is controlled by an electronic valve (EV), here, a *Bï¿½rkert* product (Type 6022). The mouth displacement is driven by a SMAC linear actuator (LAL95-050-75F/LAA-5). The water volume inside each lip is provided by a hydraulic cylinder, also driven by a SMAC linear actuator (LAL35-015-75/LAA-5). These linear actuators are all moving coils that deliver a (Laplace) force which is proportional to the input voltage. Artificial fingers are built with simple (On/Off) electromagnets. Additionally, a horn loudspeaker can be plugged at the top of the mouth, for active acoustic control issues (see [15]). The results presented below do not involve this device but its use is considered in perspectives.

Note that the inputs of these actuators are all represented and labeled at the top of figure 1.

2.3 Sensors

The position of each linear actuator (X_M for the mouth, X_{L1} and X_{L2} for the lips, see figure 2) is measured by a built-in incremental encoder with a step of $5 \times 10^{-6} m$. The (static and acoustic) air pressure in the mouth (P_M) is measured by an Endevco sensor (8507-5). A second similar sensor (8507-2) is used for the mouthpiece (P_{MP}). The (static) water pressure (P_{L1}, P_{L2}) is measured at the top of each lip (same altitude) by two Kistler sensors (RAG-25R0.5BV1H). A SMD force sensor (S215) is localized between the mouthpiece and the instrument to measure the force (F_{MP}) applied by the lips to the mouthpiece.

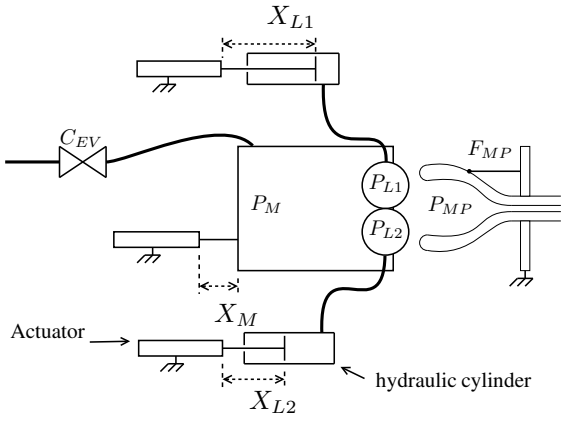

Figure 2. Sketch of the artificial mouth with its main actuators and sensors.

These sensors include built-in electronic signal conditioners except for P_M, P_{MP} and F_{MP}, which are conditioned with a low power instrumentation amplifier (INA 118). Moreover, we performed *home-made* calibrations of these sensors, except for the Endevco devices (P_M, P_{MP}) which received a factory calibration certificate. These calibrations are described in § 3.1.

Note that the outputs of the height sensors described above are all represented and labeled at the bottom of figure 1. The additional six sensors mentioned at the beginning of section 2 are: one high pressure sensor localized upstream of the electro-valve, three temperature sensors, one optical intensity sensor for estimating the opening area between the lips, and one microphone localized at the bell of the instrument. These additional sensors are not directly exploited in this paper.

2.4 Interface

The transducers associated with audio frequency ranges are connected to a sound card (see figure 3). Other transducers (with a lower frequency range) are connected to a dSpace© system, composed of an input/output interface and a Digital Signal Processor (DSP). The DSP is programmed using a dSpace software associated with a Matlab-Simulink-RTW© environment. It is used to design some (low-level) feedback loop controllers applied to the actuators. Real-time analysis of audio signals (fundamental frequencies, energy, etc) are performed by the MAX/MSP software. High-level controls of the robot (initializations, automated experiments, etc) are performed by Python scripts under the dSpace ControlDesk environment which communicates with MAX/MSP©.

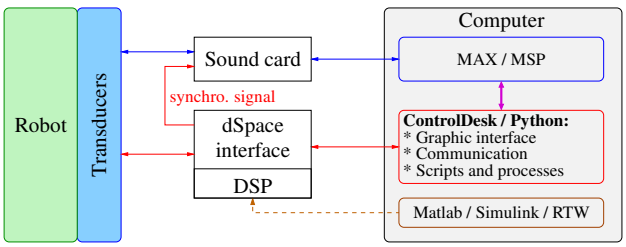

Figure 3. Overview of the interface.

3. CALIBRATION AND CONFIGURATION

The section deals with: (1) the calibration of the force sensor (F_{MP}) and the water pressure sensors (P_{L1}, P_{L2}), (2) the initialization of the *zero positions* of the linear actuators (X_{L1}, X_{L2} and X_M) so that this reference corresponds to a *robust reference state* of the lips, (3) the development and the adjustment of feedback loops to control linear actuators with respect to chosen command variables (possibly different from the natural one, the Laplace force).

3.1 Calibrations

The force and the water pressure sensors are low-frequency range sensors. We perform their calibration for quasi-static configurations. The force sensor is calibrated using gravity and reference masses (precision: $\pm 0.1g$) based on an incremental mass step of $50g$. For the water pressure sensors, a one-meter vertical water column is used, at the bottom of which the two sensors are simultaneously connected (same altitude, see figure 4). An incremental height step of five centimeters is used, corresponding to a $5 \times 10^2 Pa$ sampling precision for the pressure.

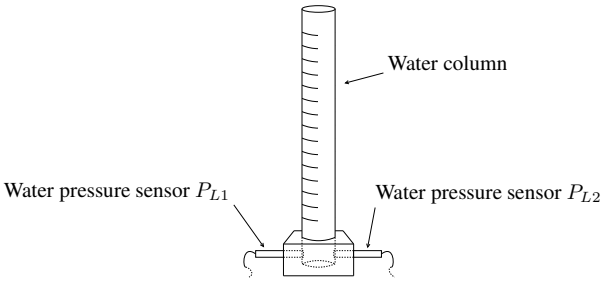

Figure 4. Schema of the water pressure sensors calibration. Static calibration based on a variable water column

The linearity of the three sensors was confirmed and the sensitivities measured.

3.2 Initialization processes

3.2.1 Zero positions for X_{L1} and X_{L2}

A lip (L) is a cylindrical latex chamber with natural volume V^{ref}. When the water volume V_L is smaller than V_L^{ref}, the latex is not stressed. In the opposite situation ($V_L > V_L^{ref}$), the latex stress makes the water pressure increase. This effect is measured by making the position X_L slowly increase from the forward to the backward trip points of the actuator[2]. We observe on the measure (see figure 5) that, except in the vicinity of V_L^{ref}, these two behaviors can be approximated by one constant pressure for $V_L < V_L^{ref}$ and an affine function with slope σ (Pa/m) for $V_L > V_L^{ref}$. The zero position of $X_L = X_L^0 = 0$ is chosen and adjusted to correspond to the intersection point of the two straight lines.

Note that $X_L = 0$ does not match with V_L^{ref}. But, it splits the curve into two affine asymptotic behaviors and defines a more robust initialization (see table 1 in § 4.2 for ten repetition tests). This initialization is performed for each lip, independently, and with no airflow.

[2] The volume variation equals the position variation multiplied by the section of the hydraulic cylinder.

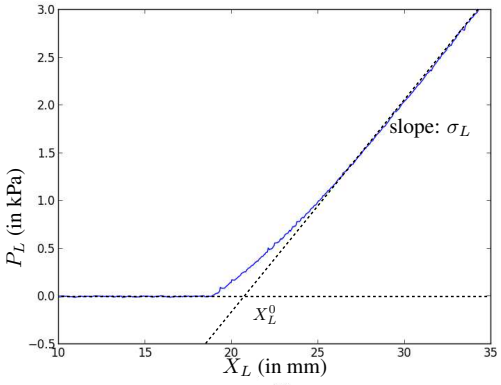

Figure 5. Measured water pressure P_{L1} with respect to the position X_{L1} when the second lip L2 is deflated and the mouthpiece is out of contact (Mouth in retracted position) and estimation of its piecewise linear approximation.

3.2.2 Zero position for X_M

Once the zero positions of the lips are estimated, that of the mouth is adjusted using a similar principle. In this case, the measured quantity is the force (F_{MP}) (rather than the water pressure) while the lips are filled with their reference volume ($X_{L1} = X_{L2} = 0$). The measurements are displayed in figure 6.

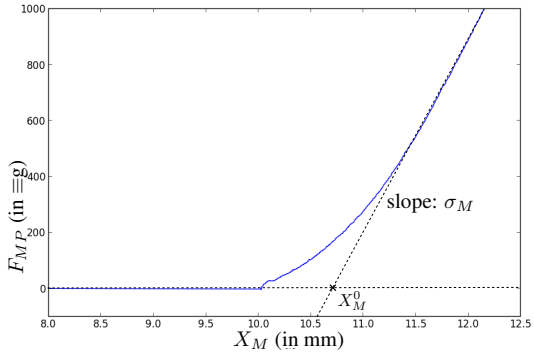

Figure 6. Measured force F_{PM} with respect to the position X_M when the lips are filled with their reference volume and estimation of its piecewise linear approximation.

Note that $X_M = 0$ does not match with the contact point between the lips and the mouthpiece, but this initialization is chosen for its robustness properties, as for $X_L = 0$.

For experiments, typical positions correspond to slightly crushed ($X_M > 0$) non over-inflated ($X_L < 0$) lips, such that the contact is established ($F_{MP} > 0$). In practice, this facilitates the formation of a buzz, or at least, that of an airflow path between the lips even for low static pressure in the mouth.

3.3 Feedback loop controllers and modes of control

The linear actuators are not naturally controlled with respect to the position but (proportionally to) the Laplace force. To achieve a control in position, we use standard tools of automatic control, here, some Proportional-Integral-Derivative (PID) controllers. Digital versions of these controllers are designed under the Matlab/Simulink/RTW environment and tuned following classical methods (see e.g. [16]). They are implemented in the DSP card of the dSpace system. For the control in position, typical performances are about 50ms. Other control types (in F_{MP}, P_{L1} or P_{L2}) are available and also based on PID controllers.

In this paper, several *modes of control* of the lips are considered. They consists of choosing, for each linear actuator, a control of *position type* or of *force/pressure type*. But, not all the combinations are compatible: positions are independent variables but, because of the contact between the lips and the mouthpiece, the force and the water pressures are linked. Here, we consider *modes of control* which include no more than one input of *force/pressure type*:

(X_M, X_{L1}, X_{L2}) this mode controls variables which do not depend of the system state;

(F_{MP}, X_{L1}, X_{L2}) this mode is well-adapted to control the contact quality between the lips and the mouthpiece;

(X_M, P_{L1}, X_{L2}) this mode (or its symmetrical version) allows the study of the effect due to the stress of one particular lip.

The feasibility of these three modes is confirmed and the repeatability is tested in section 4. Moreover, in sections 5 and 6, the two first modes are used, combined with the airflow supply, to explore self-oscillations. They allow the automatic generation of cartographies of sound descriptors, following the curves or the surfaces detailed in figure 7.

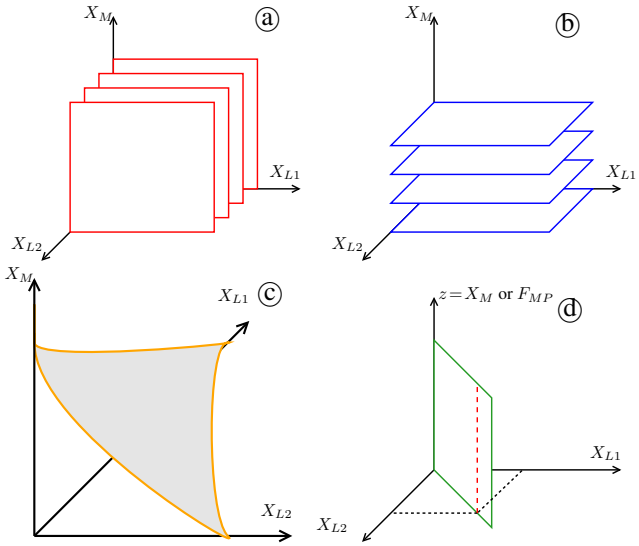

Figure 7. *Modes of control* of the three linear actuators combined with *partitions* of 3D spaces Subfigures ⓐ-ⓑ illustrate two types of partition of the 3D space into 2D planar subspaces, for the *mode of control* (X_M, X_{L1}, X_{L2}). Subfigure ⓒ illustrates a F_{MP}-constant surface. It is obtained with the mode of control (F_{MP}, X_{L1}, X_{L2}) where the first input is a fixed value. Subfigure ⓓ describes a symmetrical control of the lips ($X_{L1} = X_{L2}$) for a fixed value X_{L1} (1D-space: red dashed straight line) or on a range (2D-space: green plane). The very first exploration in § 5 is obtained by using the 1D control subspace in ⓓ with $z = F_{MP}$, and the 2D cartographies in § 6 by using the 2D spaces described in ⓐ-ⓒ and ⓓ with $z = X_M$.

4. EXPERIMENTAL PROTOCOL AND REPEATABILITY

In this section, we propose: (1) a protocol adapted to the quasi-static experiments presented in section 5 and section 6, (2) a repeatability test.

4.1 Protocol

An experiment is processed choosing a mode of control, an exploratory subspace, and following a precise protocol. The subspace is explored with quasi-static commands. To ensure quasi-static states, waiting times are added between measurements. For each measured point, every data from all sensors (Temperatures, Pressures, Positions, etc) are recorded and saved. Moreover, acoustic signals are automatically analyzed using tools provided by the MIR toolbox [17, 18]. For all measured points, sound descriptors such as fundamental frequency (if any), sound energy and roughness are estimated and saved. The protocol consists of the following steps:

1. Measurement of the idle-state of the machine
2. First initialization process: measurement of X_M^0, X_{L1}^0, X_{L2}^0, σ_M, σ_{L1} and σ_{L2}.
3. For each desired point of measurement in the subspace:
   (a) The chosen position (or force/pressure) command are set up;
   (b) First waiting: a $0.5s$ waiting is imposed to ensure actuators positions;
   (c) Breath activation: C_{EV} goes from 0 (close position) to a reference (here, 35% of the maximal aperture);
   (d) Second waiting: a $1s$ waiting is imposed to ensure a quasi- stationary regime;
   (e) Measurements are recorded and saved.
4. Second initialization process.
5. Measurement of the static pressures and the temperatures of the machine.

Parameters that are estimated during steps 2 and 4 are saved. They are compared to validate the constancy of the lips behavior. More precisely, the deviations of σ_M, σ_{L1} and σ_{L2} characterize the latex fatigue due to an experiment. The deviations of X_M^0,X_{L1}^0 and X_{L2}^0 allow the detection of anomalies such as water leaks.

Observed variable Θ	Operating Range (OR)	$Error(\Theta) * 100/OR$ (in %) by mode of control (X_M,X_{L1},X_{L2})	(F_{MF},X_{L1},X_{L2})	(X_M,P_{L1},X_{L2})
X_M	$[0\ ,\ 5\times10^{-3}]$ (in m)	$\mathbf{0.013}\%$	0.26%	$\mathbf{0.020}\%$
X_{L1}	$[0\ ,\ 3\times10^{-2}]$ (in m)	$\mathbf{5.48\times10^{-3}}\%$	$\mathbf{6.31\times10^{-3}}\%$	1.8%
X_{L2}	$[0\ ,\ 3\times10^{-2}]$ (in m)	$\mathbf{6.12\times10^{-3}}\%$	$\mathbf{6.13\times10^{-3}}\%$	$\mathbf{6.20\times10^{-3}}\%$
F_M	$[0\ ,\ 1500]$ (in g)	1.18%	$\mathbf{0.57}\%$	1.34%
P_{L1}	$[0\ ,\ 15]$ (in kPa)	1.56%	0.89%	$\mathbf{0.90}\%$
P_{L2}	$[0\ ,\ 15]$ (in kPa)	1.57%	0.96%	1.16%
P_M	$[0\ ,\ 15]$ (in kPa)	3.5%	1.45%	2.93%
Average Error		1.21%	0.59%	1.17%

Table 1. Errors relative to the operating range (OR), measured with the repeatability tests ($N_i = 10$, $N_k = 4\times4\times4 = 64$) for three modes of control. Values in bold correspond to the controlled variables.

4.2 Repeatability tests

To evaluate the repeatability of an experiment based on the protocol seen above, we perform a test for each mode of control presented in section 3. N_i identical experiments are processed. Experiments explore a set of N_k points that are fixed and distributed in the 3D-space. Between each experiment, the initialization parameters are manually disturbed: some water is added or removed in the "water circuit" and the instrument is slightly displaced (by hand).

Measurements are compared and analyzed, based on the following definitions:

1. A variable Θ measured at point k during experiment i is denoted Θ_k^i where Θ can be a *measurement* on a sensor with a low frequency range (F_{MP}, X_M, etc), or a *parameter estimated on a stationary signal* (typically, a *sound descriptor*, see below).

2. For a given point k, the expected value $E(\Theta_k)$ is estimated by its average on the N_i experiments, namely,
$$E(\Theta_k) \approx \frac{1}{N_i}\sum_{i=1}^{N_i}\Theta_k^i.$$

3. The standard deviation is correspondingly estimated by
$$s(\Theta_k) = \sqrt{E(\Theta_k^2) - E(\Theta_k)^2}.$$

4. The standard deviation of a variable Θ, averaged on the N_k experimental points, is denoted
$$Error(\Theta) = \frac{1}{N_k}\sum_{k=1}^{N_k} s(\Theta_k).$$

Results are presented in table 1 for the measurements of positions, water pressures and the force F_{MP}. In this table, to make the comparison between variables easier, the error is normalized with the (amplitude of the) operating range. The results show that the protocol and the initialization process are accurate enough to guarantee and quantify the repeatability for quasi-static experiments. Note that the mode of control based on the force (F_{MF},X_{L1},X_{L2}) appears to be, globally, the most efficient: it reduces the average error. Moreover, for this mode of control, the last step of the initialization process is not required.

5. FIRST EXPERIMENT WITH A SINGLE CONTROL VARIABLE

5.1 Global considerations

At low order, the musician's lips can be approximated by mass-damper-spring mechanical systems [4]. Here, these 3×2 macro-parameters are related to the 3 control inputs (see figure 7), making them linked together. For instance, for a fixed position X_M (figure 7, mode ⓑ), the variation of the (oscillating part of the) mass M_k of the lip Lk nearly equals that of the water displaced by X_{Lk}. The variations of stiffness K_k and damping D_k are more complex to model. Their measurement is not straightforward, even at a static equilibrium. This is why in e.g. [3, 4], these parameters are (at least partially) estimated, by analyzing the natural frequency of buzzes. In this paper, we simply explore the variability of regimes by modifying the control inputs: several frequencies can actually be reached because the sensitivities of parameters (M_k, D_k, K_k) w.r.t the control inputs are not proportional. The experiment described below makes a first exploration of regimes for a simple 1D control.

5.2 Description of the experiment

The 1D control is chosen so that the lips are in a symmetrical configuration. In order to makes this configuration as robust as possible, the independent variables $X_{L1} = X_{L2}$ are kept constant and fixed to $-15mm$, and the mouth control is chosen to be F_{MP} which increases from $100g$ to $1000g$, following the protocol described in § 4.1.

5.3 Measurements and observations

Figure 8 shows the measured force F_{MP} and signal descriptors [17, 18] of the acoustic pressure measured in the mouthpiece P_{MP}. The three sub-figures respectively display: (1) the *force*, (2) the *fundamental frequency* f_0 of P_{MP}, estimated by the YIN algorithm [18], and (3) the *energy* of the signal. An additional curve representing the *roughness* is superposed to the estimated fundamental frequency. The roughness is defined without unit: a high value means that the signal is not harmonic.

This figure validates that several fundamental frequencies are reachable. The analysis of sound descriptors clearly allows the extraction of connected areas of self-oscillating

regimes for which the roughness is low and the energy is high. These areas correspond to some *"stable notes"*. The complementary areas basically correspond to non-oscillating or complex signals (multiphonics, chaos, etc). Complex signals are mainly located in thin transition areas between stable notes.

5.4 First conclusion

This experiment shows that the robotic platform is able to produce various self-oscillating regimes including *stable notes*. For *stable notes*, it appears that, to a large extent, the higher the force F_{MP}, the higher the fundamental frequency. Moreover, stables notes and their areas are sufficiently reproducible to map some control input values to fundamental frequencies. Next section extends this exploration to the case of two control inputs.

6. TWO-DIMENSIONAL CARTOGRAPHIES

In this section, four experiments are set up, based on the modes of control ⓐ to ⓓ in figure 7.

6.1 Description of the experiments

Experiments are conducted following the protocol in § 4.1. For each experiment, the control inputs are specified below with their exploration range and the incremental step. Variables are sorted as follows: the first, second and third ones respectively correspond to (1) a *constant* value (except in case ⓓ), (2) a slow increasing sweep, and (3) a faster (but still quasi-static) increasing sweep. Parameters are:

Mode ⓐ: $X_{L2} = -15mm$; $1mm \leq X_M \leq 4mm$ (step: $0.1mm$); $-30mm \leq X_{L1} \leq 0mm$ (step: $0.5mm$);

Mode ⓑ: $X_M = 3.5mm$; $-30mm \leq X_{L2} \leq 0mm$ (step: $0.5mm$); $-30mm \leq X_{L1} \leq 0mm$ (step: $0.5mm$);

Mode ⓒ: $F_{MP} \equiv 500g$; $-30mm \leq X_{L2} \leq 0mm$ (step: $0.5mm$); $-30mm \leq X_{L1} \leq 0mm$ (step: $0.5mm$);

Mode ⓓ: $1mm \leq X_M \leq 4mm$ (step: $0.1mm$); $X_{L1} = X_{L2}$ with $-30mm \leq X_{L1} \leq 0mm$ (step: $0.5mm$).

6.2 Measurements: comments and observations

The results of these four experiments are given in figure 10. For each mode of control, ⓐ-ⓓ, connected areas associated with *"stable notes"* can still easily be extracted. However, these 2D cartographies makes some complexity appear: they include non convex areas and a large variety of sizes, specially for modes ⓐ and ⓑ. The experiment for mode ⓓ) is an extension of that shown in section 5. We can observe wide diagonal bands of *stable note* areas so that mode ⓓ makes the note selection simpler than other modes. Indeed, a preferred axis can be selected (such as X_L proportional to X_M) in order to explore areas of stable notes with increasing frequencies.

Sub-figure ⓒ displays a few number of huge or confined areas, meaning that the force is well adapted to stabilize some specific notes (here, denoted N1 and N2).

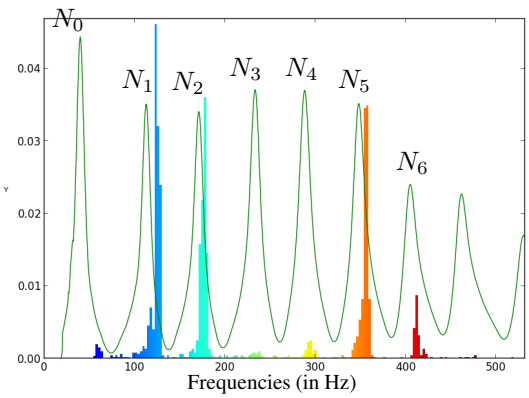

Figure 9. Normalized histogram of fundamental frequencies superposed to the modulus of the input impedance measured with the BIAS system [20].

However, note that, the symmetry with respect to lips 1 and 2 is not satisfied, although initializations are correct (and their reproducibility is checked). This can also be observed in sub-figure ⓑ. This issue will require a special attention in a future work.

Moreover, the histogram in figure 9 shows that the seven first notes of the instrument (N_0 to N_6) can be played. We can notice that playable frequencies perfectly fit with the trombone impedance (green solid line curve) but are located at the right of each peak (as expected [19]).

7. CONCLUSIONS AND PERSPECTIVES

In this paper, a robotized artificial mouth dedicated to playing the brass instruments is described with its mechatronic parts, its calibration, some robust initialization processes and several modes of control. Repeatability tests (ten acquisitions for each mode of control) is performed to estimate the standard deviation on the measured variables which characterize the lips in quasi-static configurations. Globally, the relative deviation proves to be less than 0.9% for the controlled variables and less than 3.5% for the uncontrolled ones. A protocol for experiments is proposed. In particular, it records the temperature during a (possibly long) experiment and characterizes the latex fatigue. Experiments on a trombone are designed to build cartographies for several modes of (quasi-static) control. These cartographies display sound descriptors (fundamental frequency, roughness, energy) as a function of the control input values. This exploration reveals that several stable notes can easily be reached using a basic mapping but that notes in the high range of the instrument cannot be played by the artificial mouth.

To cope with this limitation, a perspective is to modify the machine in order to make it able to play notes in the high register. A solution could consist of controlling the acoustic impedance of the mouth. A partial but encouraging result based on an acoustic active control can be found in [15]. In this work, the RMS pressure amplitude is analyzed with respect to the (controlled) phase difference between the pressure in the mouth and in the mouth-

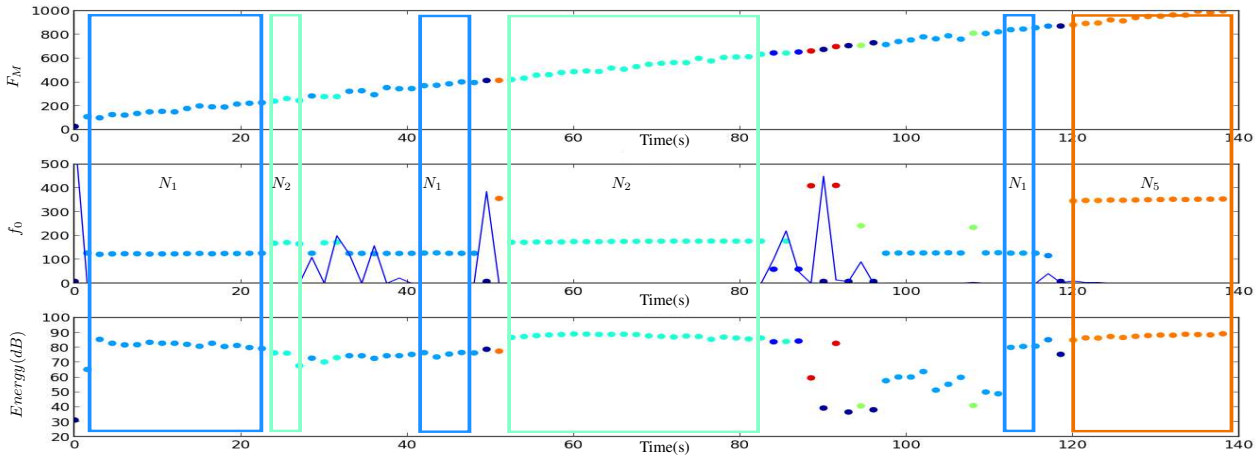

Figure 8. (First experiment: $X_{L1} = X_{L2} = -15mm$ and F_{PM} increasing from $100g$ to $1000g$) Top: F_M w.r.t. time. Middle: fundamental frequency estimated on the acoustic signal P_{MP} ($\cdot$) and roughness (-). Bottom: signal energy. In this figure, the color map corresponds to the frequencies and areas with stable notes are emphasized with boxes.

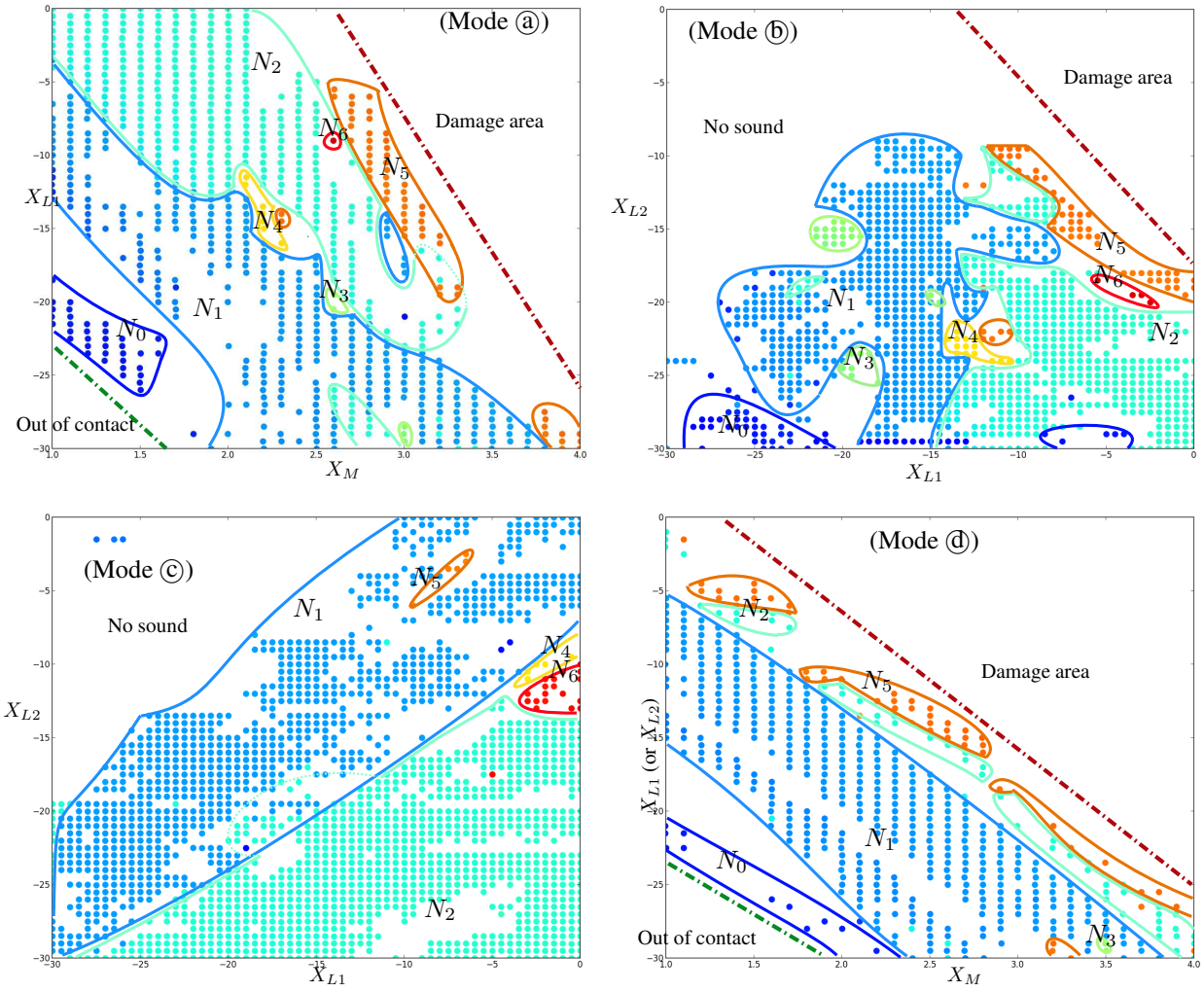

Figure 10. 2D-cartographies for various control modes. Top left: mode (X_M,X_{L1},X_{L2}) with constant X_{L2}. Top right: mode (X_M,X_{L1},X_{L2}) with constant X_M. Bottom left: mode (F_{MP},X_{L1},X_{L2}) with constant F_{MP}. Bottom right: mode (X_M,$X_{L1} = X_{L2}$). The color map corresponds to the frequencies (see figure 9) and stable note areas are surrounded. The red dotted line represents the security limit ($P_{L1} > 15kPa$ or $P_{L2} > 15kPa$) and the green dotted line represents the contact between the lips and the mouthpiece.

piece. A second perspective concerns the study of some macro-mechanical parameters of the lips (effective mass M, damping D and stiffness K) with respect to the control inputs. However, note that the (3D) control inputs do not allow the setting of the (3×2) macro-parameters. A first approach is to hold up one lip (its 1D control is then used to ensure the air-tightness). The 2D remaining control inputs can then be used to tune two of the three macro-parameters of the other (vibrating) lip, typically, M and K. A third perspective is to implement some high-level feedback loop controllers driven by the fundamental frequency and acoustic the energy.

More generally, a complete dynamical system modeling of the machine is under study. The long-term goals of this research are to: (1) derive state observers, (2) design efficient high-level controllers, and (3) build inversion processes to make the machine play target sound waves.

Acknowledgments

Authors wish to thank the French National Research Agency and the project CAGIMA for supporting this work and Alain Terrier and Gï¿½rard Bertrand for their technical assistance.

8. REFERENCES

[1] C. Vergez and X. Rodet, "Comparison of real trumpet playing, latex model of lips and computer model," in *ICMC: International Computer Music Conference*, Thessanoliki Hellas, Greece, Septembre 1997, pp. 180–187.

[2] ——, "Experiments with an artificial mouth for trumpet," in *ISMA: International Symposium of Music Acoustics*, Leavenworth, Washington state USA, Juin 1998, pp. 153–158.

[3] J. Gilbert, S. Ponthus, and J.-F. Petiot, "Artificial buzzing lips and brass instruments: experimental results," *J. Acoust. Soc. Am.*, vol. 104, no. 3, pp. 1627–1632, 1998.

[4] J. Cullen, J. Gilbert, and D. M. Campbell, "Brass instruments : linear stability analysis and experiments with an artificial mouth," *Acta Acustica united with Acustica*, vol. 86, no. 3, pp. 704–724, 2000.

[5] J.-F. Petiot, F. Teissier, J. Gilbert, and M. Campbell, "Comparative analysis of brass wind instruments with an artificial mouth: First results," *Acta Acustica united with Acustica*, vol. 89, no. 6, pp. 974–979, 2003.

[6] J. Kergomard, "Projet consonnes: Contrôle des sons naturels et synthétiques," Agence Nationale de la Recherche (ANR-05-BLAN-0097-01), 2005-2009, http://www.consonnes.cnrs-mrs.fr/.

[7] "Mechatronics projects of the engineering school of mines paristech," http://www.mecatro.fr/.

[8] B. Véricel, "Commande et interfaçage d'un robot musicien," 2009.

[9] ——, "Confrontation théorique/expérimentale de caractéristiques d'excitation dans le jeu des cuivres," 2010. [Online]. Available: http://articles.ircam.fr/textes/Vericel10a/

[10] N. Lopes, "Cartographie de paramètres de jeu de trompettiste: mise en correspondance automatique du son produit avec les paramètres de contrôle d'une bouche artificielle asservie," 2011. [Online]. Available: http://articles.ircam.fr/textes/Lopes11a/

[11] ——, "Modélisation, asservissement et commande d'une bouche artificielle robotisée pour le jeu des cuivres," 2012. [Online]. Available: http://articles.ircam.fr/textes/Lopes12a/

[12] D. Ferrand, T. Hélie, C. Vergez, B. Véricel, and R. Caussé, "Bouches artificielles asservies: étude de nouveaux outils pour l'analyse du fonctionnement des instruments à vent," in *Congrès Français d'Acoustique*, vol. 10, Lyon, France, Avril 2010. [Online]. Available: http://articles.ircam.fr/textes/Ferrand10a/

[13] T. Hélie, N. Lopes, and R. Caussé, "Robotized artificial mouth for brass instruments: automated experiments and cartography of playing parameters," in *PEVOC - Pan European Voice Conference*, vol. 9, Marseille, France, 2011, pp. 77–78.

[14] ——, "Open-loop control of a robotized artificial mouth for brass instruments," in *Acoutics 2012 (ASA)*, Hong Kong, China, 2012, pp. 1–1.

[15] V. Fréour, N. Lopes, T. Hélie, R. Caussé, and G. Scavone, "Simulating different upstream coupling conditions on an artificial trombone player system using an active sound control approach," in *International Conference on Acoustics*, vol. 21, 2013, p. 5p.

[16] K. Aström and T. Hägglund, *PID Controllers: Theory, Design, and Tuning*, 2nd ed. International Society for Measurement and Control, 1995.

[17] O. Lartillot and P. Toiviainen, "A Matlab Toolbox for Musical Feature Extraction from Audio," in *the 10th International Conference on Digital Audio Effects (DAFx07)*, 2007, pp. 237–244.

[18] A. de Cheveigné and H. Kawahara, "Yin, a fundamental frequency estimator for speech and music," *J. Acoust. Soc. Amer.*, vol. 111, pp. 1917–1930, 2002.

[19] M. Campbell, "Brass instruments as we know them today," *Acta Acustica united with Acustica*, vol. 90, pp. 600–610, 2004.

[20] G. Widholm, H. Pichler, and T. Ossmann, "Bias: A computer-aided test system for brass wind instruments," in *Audio Engineering Society Convention*, vol. 87, 1989, paper 2834.